Ultrasound-driven microbubbles for local drug delivery

Guillaume Lajoinie, Silke Roovers, Ine De Cock, Ying Luan, Erik Gelderblom, Benjamin Dollet, Heleen Dewitte, Ine Lentacker, Nico De Jong, Michel Versluis

FA2020/1108
Ultrasound-driven microbubbles for local drug delivery

G. Lajoinie[a], S. Roovers[b], I. De Cock[b], Y. Luan[c], E. Gelderblom[a], B. Dollet[d], H. Dewitte[b], I. Lentacker[b], N. De Jong[c] and M. Versluis[e]

a. University of Twente, drienerloolaan 5, 7522NB Enschede, Netherlands
b. Ghent Research Group on Nanomedicines, Ghent University, 9000 Ghent, Belgium
c. Biomedical Engineering, Thoraxcenter, 3013 Rotterdam, Netherlands
d. LIP, CNRS, 38000 Grenoble, France
e. Physics of Fluids group, Postbus 217, 7500 Twente, Netherlands
g.p.r.lajoinie@utwente.nl

ABSTRACT

Bubbles decorated with a functional payload are convenient transport vehicles and offer highly localized release. These bubbles are traceable using ultrasound and can be activated on demand. In addition, microbubbles offer an active way to mechanically overcome biological barriers. Such microbubbles are therefore being extensively investigated for single cell, gene and cancer therapy. We combine three optical imaging techniques to capture the bubble-cell interactions on timescales ranging from sub-microseconds to several seconds. We observe that non-spherically oscillating microbubbles release their nanoparticle payload in the first few ultrasound cycles. At low pressures, the released nanoparticles are transported away by microstreaming, as observed for single microbubbles. Higher pressures (> 300 kPa) and longer ultrasound pulses (>100 cycles) lead to rapid translation of the microbubbles and transport of the released nanoparticles in the microbubbles wake, eventually leading to the deposition of nanoparticles in elongated patches onto the cell membrane.

1. INTRODUCTION

Ultrasound is a leading imaging modality in the clinics owing to its excellent safety record, high resolution, and penetration depth. However, it lacks specificity. Microbubble ultrasound contrast agents are designed to increase both specificity and sensitivity by acting as strong nonlinear point sources. More specifically, these agents consist of microbubbles with a size between 1 to 3 μm. When exposed to an ultrasound wave, they show a strong resonance behavior whose eigenfrequency, as predicted by Minnaert **[1]**, is inversely proportional to the radius. This unique property has been exploited for decades for clinical diagnosis. Driven near its resonance frequency, a bubble oscillates strongly and nonlinearly, generating both harmonics and subharmonics frequencies **[2,3]**, exerting acoustic radiation forces, and displaying shape instabilities **[4]** and non-spherical oscillations **[5,6]**. When injected, microbubbles must travel the blood stream for up to a minute before reaching the area of interest. To provide sufficient stability, microbubbles are therefore coated with polymers, proteins, or lipids. Phospholipids are by far the most commonly used owing to their high biocompatibility and non-linear acoustic properties **[7]**. Furthermore, lipid coatings can readily be decorated with ligands that specifically adhere to diseased cells and tissues **[8,9]** Alternatively, these ligands can also be used to load the microbubbles with various molecules **[10,11]** and nanoparticles such as RNA-loaded liposomes or chemotherapeutic particles **[12,13].** The payload is then protected from the natural clearing mechanisms of the body. This loading, in combination with the unique resonance of the bubbles, is of prime importance in biofilms removal **[14]**, thrombolysis **[15]**, tumors lysis **[16,17]** or inducing vessel wall permeation **[18]**. Experimental investigation of microbubble interactions with cell monolayers has led to the description of a phenomenon termed “sonoprinting”: confocal imaging shows how exposure of the microbubbles to ultrasound can result in the deposition of their payload in patches onto the cell membrane. In parallel, investigation of single microbubbles suggests that the payload is released in the opposite direction. To reconcile these observations, it is critical to understand the mechanisms by which this payload is released from the microbubble carriers and delivered to cells or. Several theories have been proposed to explain the shedding of the microbubble shell: Borden et al. **[19]** suggested that the expulsion of excessive shell material during compression was a direct result of surface area reduction. O'Brien et al. **[20]** proposed to consider the shedding as a resulting from molecular viscosity. Finally, Kwan et al. **[21]** concluded that the release could originate from a cyclic generation of lipid folding events. However, a cyclic process is difficult to combine with the experimental evidence that shedding occurs within just a few ultrasound cycles **[22]**. Overall, these theories are difficult to demonstrate owing to the sub-microsecond timescale and sub-micrometer length scale of the problem. To revisit this problem experimentally, we combine three optical imaging techniques to capture the bubble-cell interactions on timescales ranging from sub-microseconds to several seconds. Single-bubble experiments demonstrate how non-spherical bubble oscillations induce both, the release of the drug payload and its transport by microbubble-induced streaming. These observations are validated with a simple model. When combining the bubbles with cells, we observe that,

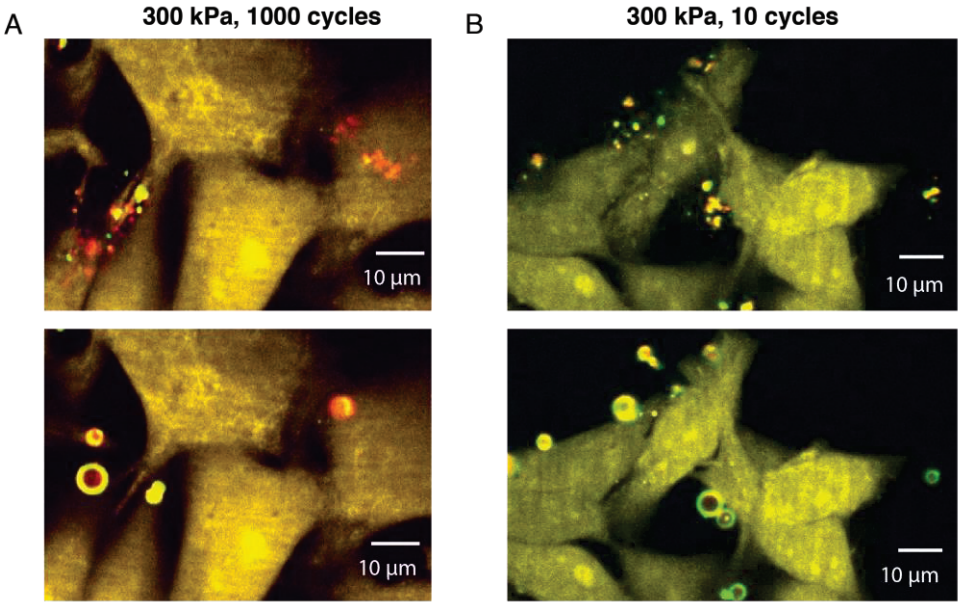

Figure 1: Confocal imaging snapshots taken just before (top panels) and just after (bottom panels) for an ultrasound pressure of 300 kPa and a pulse length of 1000 cycles (A) and 10 cycles (B).

at low pressures, the released nanoparticles are transported away by microstreaming, as observed for single microbubbles. This configuration, however, sends the drug payload away from the membrane and therefore does not favor of nanoparticle uptake by the cells on the membranes. However, higher pressures (> 300 kPa) and longer ultrasound pulses (> 100 cycles) lead to rapid translation of the microbubbles and transport of the released nanoparticles in the microbubbles wake, eventually leading to the deposition of nanoparticles in elongated patches onto the cell membrane.

2. ULTRASOUND-INDUCED SONOPRINTING

The use of confocal imaging allows for high-resolution imaging of the cell response to the microbubble oscillation. To that end, the microbubbles shell is labeled with red DiD dye that intercalates between the phospholipids, and the liposomes are labeled with green-fluorescent cholesteryl-BODIPY™ FL C12 dye. In addition, the cells are labeled with CellTrace™ Yellow to delineate them and detect potential disruptions of the membranes. Figure 1 displays typical examples of the response of a cell monolayer to the microbubble oscillation upon excitation with a 300 kPa ultrasound burst. For a burst length of 10 cycles (Fig. 1B), the bubbles release their cargo in the vicinity of the cells, but the material is not directly delivered to the cell and floats in the medium. For a pulse length of 1000 cycles at the same pressure, however, the drug payload it deposited in patches onto the cell membrane. This is the mechanism termed “sonoprinting”. There, the patches are static, and clearly adherent to the cell membrane. In both cases, there is clear evidence of membrane damage. Note that the red and yellow dyes remain largely collocated, showing that the phospholipid shell of the microbubble is released at the same time as the drug payload.

It is very clear that the fate of the drug payload depends on the ultrasound settings and bubbles properties. It is also clear that the mechanism leading to sonoprinting is of far greater interest, since it couples the therapeutics to the cells directly, opening the way to endocytosis and in general uptake by the cell. In contrast, the release of free material in the surrounding of the cell is less interesting: since microbubbles are blood-pool agent, it is reasonable to expect that the release will involve vessel-lining cells and, therefore, a freely floating drug would simply be washed away.

3. SINGLE-BUBBLE RELEASE

Understand the mechanisms that lead to a positive outcome it terms of sonoprinting is therefore of utmost importance. To understand the response of drug-loaded bubbles to ultrasound, we combine ultra-high-speed bright-field imaging at 5 million frames per second and high-speed fluorescence imaging at 50.000 frames per second. Furthermore, the experiments are performed in side-view to capture the plane of symmetry of the system since the bubbles are floating against a polymer membrane. These experiments provide a surprisingly consistent behavior: upon insonation, the microbubble oscillate in a non-spherical way (see Fig. 2A), which can be quantitatively simulated using a simple model based on the Rayleigh-Plesset equation. The origin of these oscillations lies in the presence of the polymer membrane. The details of this model can be found in [23]. In short, the bubble is discretized in angular segments whose dynamics follows the Rayleigh-Plesset equation. These multiple oscillators are then coupled by the gas pressure and the local curvature of the bubble.

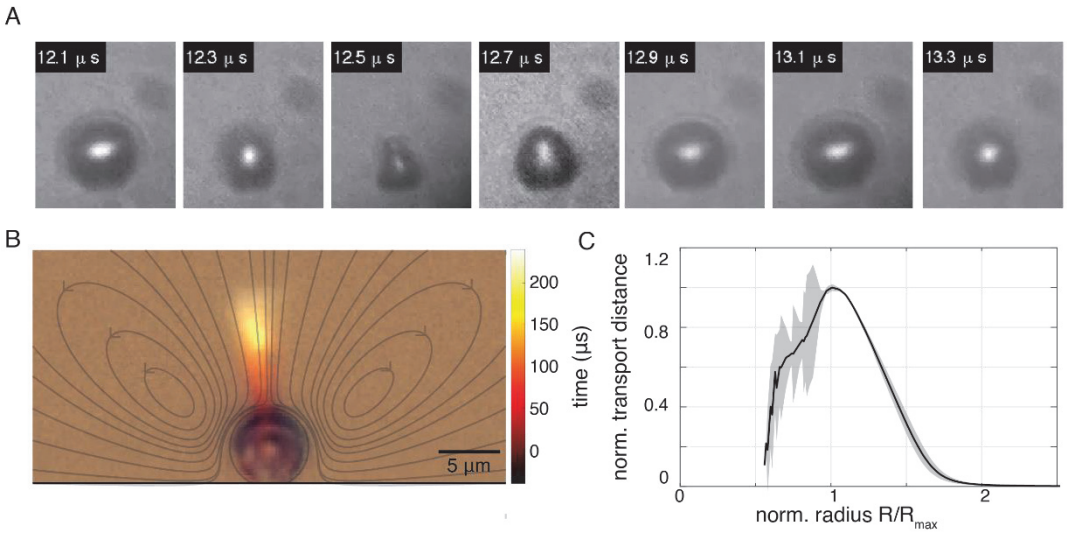

Figure 2: A. Still frames from a side-view, bright-field optical recording performed at 5 million frames per second. The pictures depict a full ultrasound period. B. High-speed fluorescence imaging showing the release and transport of the payload from the microbubble surface. The bubbles shell is labeled with a fluorescent dye. The original recording was performed at 50.000 frames per second. The theoretical streamlines corresponding to the streaming generated by the microbubbles are materialized by the solid grey lines. C. normalized transport distance, away from the microbubbles as a function of the normalized bubbles radius. The radius is normalized by the radius of maximum response of the microbubble.

Interestingly, the resulting non-spherical oscillations result in the generation of microstreaming, as was described in [24]. The streamlines closest to the bubble surface are directed directly upwards and the flow take with it the material that detaches from the bubble surface as can be seen in Fig. 2B. Fig. 2B is an overlay of a high-speed fluorescence recording where the color encodes the time. The material is already released from the bubble shell after a few microseconds and is transported over a distance larger than the bubble itself over a time span of 200 µs. The transport of the shell material in these conditions is predictable and follows the curve displayed in Fig. 2C. The grey area in Fig. 2C represents the uncertainty in the simulated response of small bubbles for different acoustic pressures, owing to a limited numerical stability in this region. Interestingly, the radius at which most transport is observed is not directly the resonant radius because of the complex and nonlinear phenomena giving rise to the streaming and subsequent transport. A fit provides an estimate of the radius of maximum response and transport distance. Interestingly, although the streaming increases quadratically with the acoustic pressure, the distance over which the material is transported increases linearly with the acoustic pressure.

4. RECONCILING SINGLE-BUBBLE EXPERIMENTS WITH SONOPRINTING

Figure 1 shows that bubbles can display two distinct behavior when they interact with cells. In particular, they can print their payload onto cell membranes. However, single bubbles are consistently observed to induce streaming and release their payload in one direction, namely away from the nearby membrane. To reconcile these observations, we perform a new set of experiments where the response of bubbles in the presence of cells is recorded using hybrid high-speed imaging that superposes bright-field and fluorescence microscopy **[25]**. This technique allows to visualize the cells, the bubbles gas cores, and the fluorescent payload simultaneously. 2 distinct behavior are observed. For low pressure and short cycles, the release is dominated by streaming, as was observed during the single-bubble experiments. However, as the pulse length and pressure increase, the complexity of the environment starts to influence the dynamics of the microbubbles. Specifically, the presence of the membrane and the relative proximity of other bubbles gives rise to acoustic radiation forces, also known as Bjerknes forces. These Bjerknes forces induce a net force on the bubble toward the membrane and toward the other bubbles, This, in turn, results in a fast translation of the microbubble core, while microstreaming is generated. When the translation velocity of the bubble increases beyond that of the streaming, sonoprinting occurs. Across the parameter space, two regions exist where either streaming dominates (see Fig. 3C left panel) or sonoprinting dominates (see Fig. 3C right panel). The latter regime is of great interest for therapeutic application.

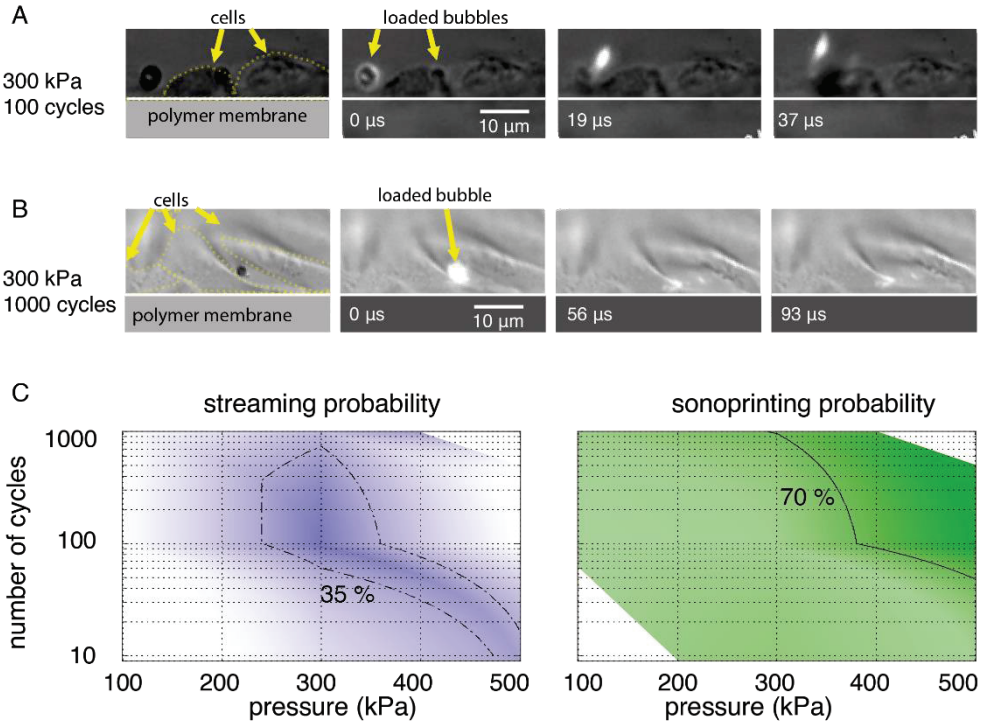

Figure 3: A. Combined bright-field and fluorescence recording of the drug release from a loaded microbubble in the vicinity of cells performed at 54.000 frames per second. The microbubble, at t=0, is exposed to an ultrasound burst of 300 kPa pressure and 100 cycles duration. B. Similar recording of a loaded microbubble exposed to an ultrasound burst of 300 kPa pressure and 1000 cycles duration. C. phase diagram pulse length versus acoustic pressure showing the regimes where the release of the payload is dominated by streaming (left) or sonoprinting (right).

5. DISCUSSION

The results reported here are acquired in the presence of a polymer membrane that, although common in in vitro work, does not constitute a relevant biological element. Since the phenomena observed are influenced by this membrane, it is valuable to investigate how these mechanisms change when bubbles interact with a 3D structure such as a spheroid. Investigations are currently ongoing in this direction **[26]**.

It is clear the translation of the gas core is responsible for sonoprinting. It is, however, less clear how this translation practically results in the observed patching. We hypothesize that, while the gas core translates, the released material is trapped in a different streamline, and recirculates towards the bubble before being eventually deposited onto the cells. There is nonetheless no evidence to confirm or invalidate this proposition.

The phase diagram proposed in Fig. 3C was realized based on relatively low amount of data as compared to the range variation of the parameters investigated. It is therefore meant as indicative and should be further refined.

This study does not consider the actual intake of drugs by the cells, which can occur in multiple way, e.g. endocytosis or diffusion through pores (sonoporation). Ultimately, these biophysical phenomena will have to be taken into consideration to achieve effective, in vivo drug delivery.

6. CONCLUSION

The interaction of drug-loaded microbubbles with cells is a complex problem, even for cell monolayers. The results shown here shed some light on the possible acoustic and fluid dynamical interactions between the bubble and their environment that may greatly influence the outcome of drug delivery. In particular, understanding the non-spherical and nonlinear bubble oscillations combined with acoustic radiation forces is critical to control drug delivery and was shown to result in two distinct regimes where the drug is either freely-floating or sonoprinted onto the cell membranes.

7. REFERENCES

[1] Minnaert, M. “On musical air-bubbles and the sound of running water”. *Philos. Mag.* 16, pp. 235-248, 1933

[2] Hope Simpson, D., Chin, C. T., Burns & P. N. “Pulse inversion Doppler: a new method for detecting nonlinear echoes from microbubble contrast agents”. *IEEE T. Ultrason. Ferr.* 46, 372-382, 1999

[3] Sirsi, S., Feshitan, J., Kwan, J., Homma, S. & Borden, M. “Effect of microbubble size on fundamental mode high frequency ultrasound imaging in mice”. *Ultrasound Med. Biol.* 36, 935-948, 2010

[4] Versluis, M. et al. “Microbubble shape oscillations excited through ultrasonic parametric driving”. *Phys. Rev. E* 82, 2010

[5] Dollet, B. et al. “Nonspherical oscillations of ultrasound contrast agent microbubbles”. *Ultrasound Med. Biol.* 34, 1465-1473, 2008

[6] Vos, H. J., Dollet, B., Versluis, M. & de Jong, N. “Nonspherical shape oscillations of coated microbubbles in contact with a wall”. *Ultrasound Med. Biol.* 37, 935-948, 2011

[7] Overvelde, M. et al. “Nonlinear shell behavior of phospholipid-coated microbubbles”. *Ultrasound Med. Biol.* 36, 2080-2092, 2010

[8] Lindner, J. R. et al. “Noninvasive ultrasound imaging of inflammation using microbubbles targeted to activated leukocytes”. *Circulation* 102, 2745-2750, 2000

[9] Klibanov, A. L. et al. “Detection of individual microbubbles of ultrasound contrast agents: imaging of free-floating and targeted bubbles”. *Invest. Radiol.* 39, 187-19, 2004

[10] Tinkov, S. et al. “New doxorubicin-loaded phospholipid microbubbles for targeted tumor therapy: In-vivo characterization”. *J. Control. Release* 148, 368-372, 2010

[11] Lentacker, I., Geers, B., Demeester, J., De Smedt, S. C. & Sanders, N. N. “Design and evaluation of doxorubicin-containing microbubbles for ultrasound-triggered doxorubicin delivery: cytotoxicity and mechanisms involved”. *Mol. Ther.* 18, 101-108, 2009

[12] Geers, B. et al. “Self-assembled liposome-loaded microbubbles: The missing link for safe and efficient ultrasound triggered drug-delivery”. *J. Control. Release* 152, 249-256, 2011

[13] Kheirolomoom, A. et al. “Acoustically-active microbubbles conjugated to liposomes: Characterization of a proposed drug delivery vehicle”. *J. Control. Release* 118, 275-284, 2007

[14] Fernandez Rivas, D. et al. “Localized removal of layers of metal, polymer, or biomaterial by ultrasound cavitation bubbles”. *Biomicrofluidics* 6, 34114, 2012

[15] Petit, B. et al. "In vitro sonothrombolysis of human blood clots with BR38 microbubbles”. *Ultrasound Med. Biol.* 38, 1222-1233, 2012

[16] Li, T. et al. “Passive cavitation detection during pulsed HIFU exposures of ex vivo tissues and in vivo mouse pancreatic tumors”. *Ultrasound Med. Biol.* 40, 1523-1534, 2014

[17] Graham, S. M. et al. “Inertial cavitation to non-invasively trigger and monitor intratumoral release of drug from intravenously delivered liposomes”. *J. Control. Release* 178, 101-107, 2014

[18] Lipsman, N. et al. “Initial experience of blood-brain barrier opening for chemotherapeutic-drug delivery to brain tumours by MR-guided focused ultrasound”. *Neuro-Oncology* 19, vi9, 2017

[19] Borden, M. A. et al. “Influence of lipid shell physicochemical properties on ultrasound-induced microbubble destruction”. *IEEE Trans. Ultrason. Ferroelec. Freq. Contr.* 52, 1992-2002, 2005

[20] O'Brien, J. P., Stride, E. & Ovenden, N. “Surfactant shedding and gas diffusion during pulsed ultrasound through a microbubble contrast agent suspension”. *J. Acoust. Soc. Am.* 134, 1416-1427, 2013

[21] Kwan, J. J. & Borden, M. A. “Lipid monolayer collapse and microbubble stability”. *Adv. Colloid Interf. Sci.* 183, 82-99, 2012

[22] Luan, Y. et al. “Lipid shedding from single oscillating microbubbles”. *Ultrasound Med. Biol.* 40, 1834-1846, 2014

[23] G. Lajoinie et al. “Non-spherical oscillations drive the ultrasound-mediated release from targeted microbubbles”, *Nat. Comms. Phys.* 1, 22, 2018

[24] Marmottant, P. & Hilgenfeldt, S. “Controlled vesicle deformation and lysis by single oscillating bubbles”. *Nature* 423, 153-156, 2003

[25] S. Roovers et al. “Sonoprinting of nanoparticle-loaded microbubbles: Unraveling the multi-timescale mechanism”. *Biomaterials* 217, 119250, 2019

[26] S. Roovers et al. “Sonoprinting liposomes on tumor spheroids by microbubbles and ultrasound”, *J. Control. Release* 316, 2019.